Journal of Molecular Structure 1012 (2012) 105–112

Contents lists available at SciVerse ScienceDirect

Journal of Molecular Structure

journal homepage: www.elsevier.com/locate/molstruc

Study on molecular structure and vibrational spectra of (triphenylphosphoranylidene) acetaldehyde using DFT: A combined experimental and quantum chemical approach

Ö. Dereli [a,*], Y. Erdogdu [b], M.T. Gulluoglu [b]

[a] A. Keleşoğlu Education Faculty, Department of Physics, Selcuk University, Meram, 42090 Konya, Turkey
[b] Department of Physics, Ahi Evran University, 40040 Kirsehir, Turkey

ARTICLE INFO

Article history:
Received 1 November 2011
Received in revised form 21 December 2011
Accepted 27 December 2011
Available online 4 January 2012

Keywords:
(Triphenylphosphoranylidene)
acetaldehyde
FT-IR
FT-Raman
DFT
Vibrational spectra
PED

ABSTRACT

In the present study, an exhaustive conformational search of the (triphenylphosphoranylidene) acetaldehyde has been performed. The FT-IR spectrum of this compound was recorded in the region 4000–400 cm^{-1}. The FT-Raman spectrum was also recorded in the region 3500–50 cm^{-1}. Vibrational frequencies of the title compound have been calculated by B3LYP method using 6-311++G(d,p) basis sets. The calculated geometric parameters and vibrational frequencies were analyzed and compared with obtained experimental results.

1. Introduction

Triphenylphosphonium compounds and their various derivatives are key reagents in the wittig reactions and they are used to convert aldehydes and ketones into alkenes [1,2], specifically in applications ranging from the synthesis of simple alkenes to the construction of complex biologically active molecules in the pharmaceutical researches [3–9]. They are also important class of isoaromatic compounds and have widespread applications in antimicrobial and anticancer activity [10–18]. In addition, phosphonium compounds enhance flame retardancy mainly in textile industry [19].

Infrared and Raman spectroscopy is an efficient method to probe electronic and geometric structure of molecules, and has been widely used in studying the structural consequences. Moreover, vibrational spectroscopy is very important for investigation of inter- and intra-molecular interactions. The *ab initio* vibrational assignments of the infrared and Raman spectrum of molecules have been widely studied for structural investigations nowadays. In recent years density functional theory (DFT) methods have become a powerful tool in the investigation of molecular structures and vibrational spectra, especially B3LYP method has been widely used [20–29]. There are very few studies about structure and vibrations of triphenylphosphonium compounds in the literature [30]. (Triphenylphosphoranylidene) acetaldehyde (TPA) is an important derivative of triphenylphosphonium compounds. The molecular structure of this compound has been studied by single crystal X-ray diffraction method previously [31]. To the best of our literature survey, there is no complete vibrational and conformational analysis data on TPA molecule in the literature.

In the present paper, an exhaustive conformational search of the TPA has been performed by molecular mechanic calculations. Geometry parameters and vibrational frequencies of the title compound have been calculated by B3LYP method using 6-311++G(d,p) basis sets. The calculated geometric parameters and vibrational frequencies were analyzed and compared with obtained experimental results.

2. Experimental

The TPA powder was purchased from Fluka. FT-IR spectrum of solid TPA was recorded in the range 4000–400 cm^{-1} on Brucker IFS 66/S with PIKE Gladi ATR (Diamond) spectrometer at room temperature with 2 cm^{-1} resolution. The FT-Raman spectrum was recorded on a Brucker FRA 106/S spectrometer using 1064 nm excitation from a Nd:YAG laser. The detector was a Ge-diode cooled to liquid nitrogen temperature. The upper limit for

* Corresponding author. Tel.: +90 533 556 9111; fax: +90 332 323 8225.
E-mail address: odereli@selcuk.edu.tr (Ö. Dereli).

0022-2860/$ - see front matter © 2012 Elsevier B.V. All rights reserved.
doi:10.1016/j.molstruc.2011.12.040

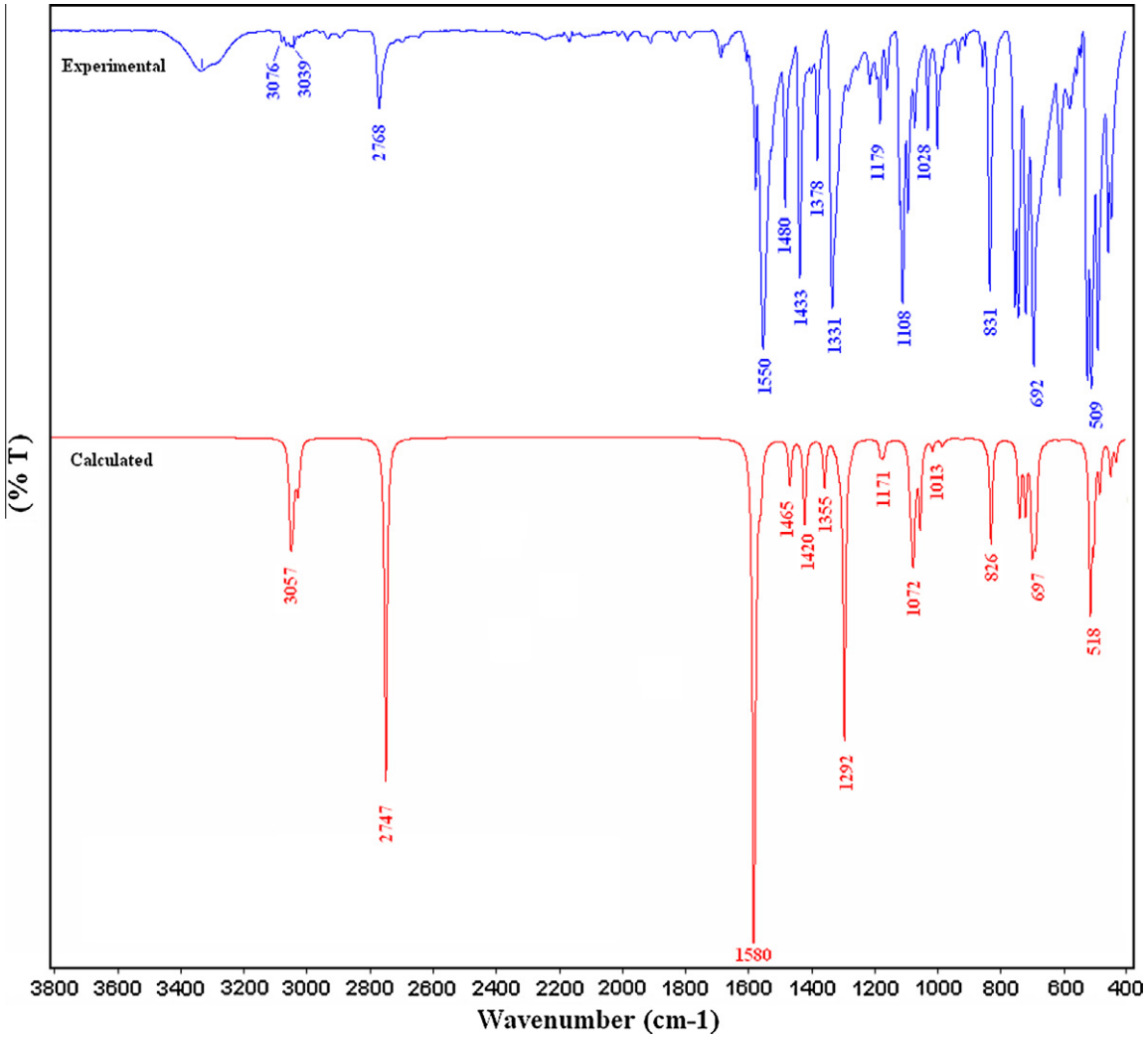

Fig. 1. Experimental and theoretical FT-IR spectra of TPA.

wavenumbers was 3500 cm^{-1} and the lower wavenumber is around 50 cm^{-1}. The measured FT-IR and FT-Raman spectra are shown in Figs. 1 and 2.

3. Computational details

In order to establish the stable possible conformations, the conformational space of TPA was scanned with molecular mechanic calculations. This calculation was performed with the Spartan 08 program [32]. In the second step, geometry optimizations of all of the possible conformers was performed by B3LYP method with 6-311++G(d,p) basis set. After the most stable conformer of the title compound determined, optimized structural parameters of this conformer were used for the vibrational frequency calculations. Optimizations and frequency calculations were performed by the same level of DFT. In this step, all the calculations were performed using Gaussian 03W program package [33] with the default convergence criteria without any constraint on the geometry [34]. The assignments of the calculated wavenumbers are aided by the animation option of Gauss View 3.0 graphical interface for Gaussian programs, which gives a visual presentation of the shape of the vibrational modes along with available related molecules [35]. Furthermore, total energy distribution (PED) was calculated by using the scaled quantum mechanic program (SQM) and fundamental vibrational modes were characterized by their PED [36].

The Raman activities (S_i) calculated with Gaussian 03 program and they were converted to relative Raman intensities (I_i) using the following relationship derived from the intensity theory of Raman scattering.

$$I_i = \frac{f(\upsilon_0 - \upsilon_i)^4 S_i}{\upsilon_i[1 - \exp(hc\upsilon_i/kT)]} \quad (1)$$

where υ_0 is the exciting frequency in cm^{-1}, υ_i the vibrational wavenumber of the (ith) normal mode, h, c and k fundamental constants, and f is a suitably chosen common normalization factor for all peak intensities [37].

4. Results and discussion

4.1. Conformational stability

To found stable conformers, a meticulous conformational analysis was carried out for the title compound. Rotating at each 10° intervals around the free rotation bonds, conformational space of the title compound was scanned by molecular mechanic calculations and then full geometry optimizations of obtained structures were performed by B3LYP/6-311++G(d,p) method. Results of geometry optimizations indicated that the title compound has two conformers as shown in Fig. 3. Ground state energies, zero

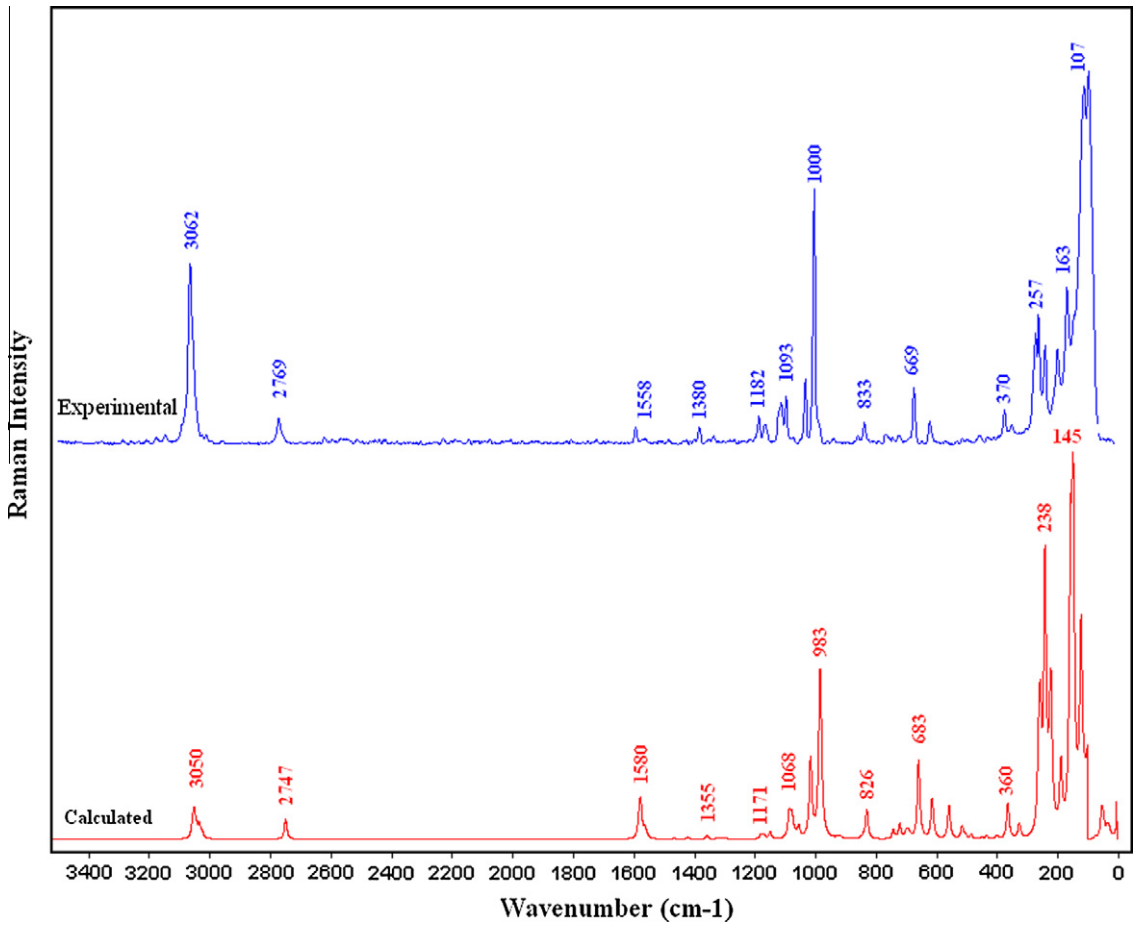

Fig. 2. Experimental and theoretical FT-Raman spectra of TPA.

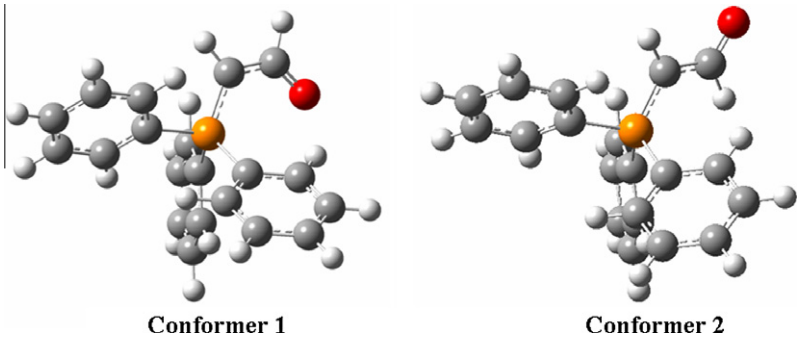

Fig. 3. Stable conformers of TPA.

point corrected energies, relative energies and dipole moments of conformers were presented in Table 1. Zero point corrections have not caused any significant changes in the stability order. From both calculated energies of two conformers, given in Table 1, the conformer 1 is the most stable and the comparison of the theoretical and experimental geometry of the title compound, given in Table 2, shows that optimized geometry of conformer 1 (namely conformer 1 appears in the solid state) fairly well reproducing the experimental one. For these reasons, from this point the discussion will be based on conformer 1, further in this paper.

Table 1
Energetics of the conformers of TPA.

Conf.	E (Hartree)	ΔE (kcal/mol)	E_0 (Hartree)	ΔE_0 (kcal/mol)	Dip. mom. (D)
1	−1189.150409	0	−1188.844282	0	5.5321
2	−1189.139569	6.802	−1188.837412	4.311	7.9967

E_0, Zero point corrected energy.

Table 2
The calculated geometric parameters of TPA by B3LYP/6-311++G(d,p) method, bond lengths in angstrom (Å) and angles in degrees (°).

Parameters	Calculated	Experimental[a]	Parameters	Calculated	Experimental[a]
Bond lengths (Å)			Bond angles (°)		
C_1—P_3	1.732	1.709	P_3—C_{15}—C_{16}	119.0	119.5
C_1—C_{37}	1.409	1.384	P_3—C_{15}—C_{17}	121.3	122.9
P_3—C_4	1.835	1.800	C_{16}—C_{15}—C_{17}	119.7	117.6
P_3—C_{15}	1.839	1.798	C_{15}—C_{16}—C_{18}	119.6	119.2
P_3—C_{26}	1.831	1.816	C_{15}—C_{17}—C_{20}	120.2	121.7
C_4—C_5	1.398	1.354	C_{16}—C_{18}—C_{22}	120.6	123.0
C_4—C_6	1.400	1.365	C_{17}—C_{20}—C_{22}	120.1	120.2
C_5—C_7	1.392	1.388	C_{18}—C_{22}—C_{20}	119.9	118.3
C_6—C_9	1.393	1.377	P_3—C_{26}—C_{27}	121.8	122.0
C_7—C_{11}	1.394	1.353	P_3—C_{26}—C_{28}	118.8	116.0
C_9—C_{11}	1.394	1.358	C_{27}—C_{26}—C_{28}	119.4	122.0
C_{15}—C_{16}	1.404	1.379	C_{26}—C_{27}—C_{29}	120.2	119.7
C_{15}—C_{17}	1.401	1.389	C_{26}—C_{28}—C_{31}	120.2	118.3
C_{16}—C_{18}	1.393	1.380	C_{27}—C_{29}—C_{33}	120.2	118.5
C_{17}—C_{20}	1.394	1.379	C_{28}—C_{31}—C_{33}	120.2	119.5
C_{18}—C_{22}	1.395	1.359	C_{29}—C_{33}—C_{31}	119.9	122.3
C_{20}—C_{22}	1.393	1.357	C_1—C_{37}—O_{39}	126.7	126.7
C_{26}—C_{27}	1.398	1.348	Selected dihedral angles (°)		
C_{26}—C_{28}	1.403	1.386	C_{37}—C_1—P_3—C_4	57.9	53.7
C_{27}—C_{29}	1.395	1.401	C_{37}—C1—P_3—C_{15}	65.1	67.6
C_{28}—C_{31}	1.392	1.391	C_{37}—C_1—P_3—C_{26}	176.1	173.8
C_{29}—C_{33}	1.393	1.358	P_3—C_1—C_{37}—O_{39}	2.7	0.5
C_{31}—C_{33}	1.395	1.371	C_1—P_3—C_4—C_5	24.9	28.3
C_{37}—O_{39}	1.243	1.249	C_1—P_3—C_4—C_6	156.4	154.9
Bond angles (°)			C_{15}—P_3—C_4—C_5	154.2	155.6
P_3—C_1—C_{37}	121.4	125.3	C_{15}—P_3—C_4—C_6	27.0	27.6
C_1—P_3—C_4	113.9	113.5	C_{26}—P_3—C_4—C_5	92.7	90.4
C_1—P_3—C_{15}	117.0	115.8	C_{26}—P_3—C_4—C_6	86.0	86.4
C_1—P_3—C_{26}	106.4	106.7	C_1—P_3—C_{15}—C_{16}	50.2	50.0
C_4—P_3—C_{15}	105.1	104.8	C_1—P_3—C_{15}—C_{17}	129.8	130.1
C_4—P_3—C_{26}	107.4	109.0	C_4—P_3—C_{15}—C_{16}	77.2	75.9
C_{15}—P_3—C_{26}	106.4	106.8	C_4—P_3—C_{15}—C_{17}	102.8	104.0
P_3—C_4—C_5	118.6	119.8	C_{26}—P_3—C_{15}—C_{16}	169.0	168.5
P_3—C_4—C_6	121.6	121.4	C_{26}—P_3—C_{15}—C_{17}	11.0	11.6
C_5—C_4—C_6	119.7	118.7	C_1—P_3—C_{26}—C27	127.8	119.5
C_4—C_5—C_7	120.1	120.2	C_1—P_3—C_{26}—C_{28}	51.6	58.7
C_4—C_6—C_9	120.0	120.8	C_4—P_3—C_{26}—C_{27}	5.4	3.4
C_5—C_7—C_{11}	120.1	120.2	C_4—P_3—C_{26}—C_{28}	174.0	178.3
C_6—C_9—C_{11}	120.1	120.4	C_{15}—P_3—C26—C_{27}	106.7	116.1
C_7—C_{11}—C_9	120.0	118.9	C_{15}—P_3—C_{26}—C_{28}	73.9	65.6

[a] X-ray data taken from Ref. [31].

4.2. Molecular geometry

Experimentally observed structural parameters of the title compound and theoretically calculated structural parameters of the most stable conformer were tabulated in Table 2 in accordance with the atom numbering scheme given in Fig. 4. Based on our calculations, all results are well correlated. A small difference between experimental and calculated geometrical parameters may come from the environment of the compound. It is clear that the experimental results belong to solid phase while theoretical calculations belong to gaseous phase. As it is seen from Table 2 and Fig. 4, the dihedral angle P3—C1—C37—O39 = 0.5° and conjugation effects can be seen between aldehyde group and —P—CH moiety of TPA.

4.3. Vibrational assignments

The TPA molecule has 39 atoms, which possess 111 normal modes of vibrations. All vibrations are active both in Raman and infrared spectra. Usually the calculated harmonic vibrational wavenumbers are higher than the experimental ones, because of the anharmonicity of the incomplete treatment of electron correlation and of the use of finite one-particle basis set [24]. The harmonic frequencies were calculated by B3LYP method using 6-311++G(d,p) basis set and then scaled by 0.967 (for wavenumbers under 1800 cm^{-1}) and 0.955 (for those over 1800 cm^{-1}) [38].

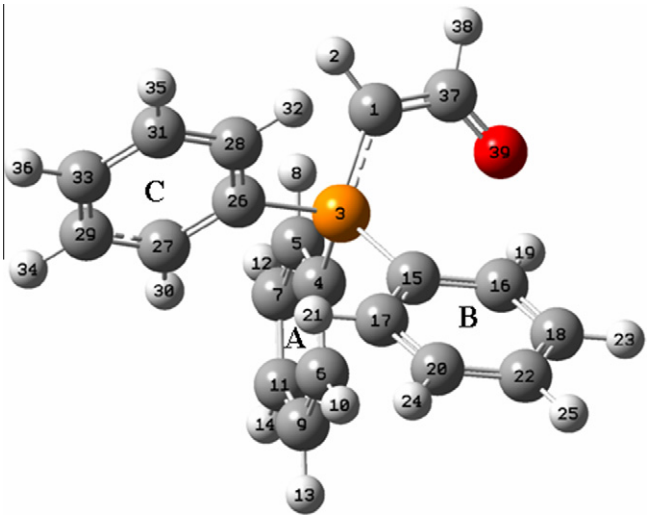

Fig. 4. Molecular structure and atom numbering scheme adopted in this study for TPA.

Experimentally observed and theoretically calculated harmonic vibrational frequencies and their correlations were gathered in Table 3. From the calculations, the computed values are in good agreement with the observed values. Deviations from the

Table 3
Comparison of the observed and calculated vibrational spectra.

Mode nos.	Experimental wavenumbers (cm^{-1})		Theoretical wavenumbers (cm^{-1}) B3LYP				Assignments PED[c] (%)
	IR	Raman	Unscaled[a]	Scaled[b]	I_{IR}	I_{RAMAN}	
1	3076 w	–	3201	3057	0	1	99υCH
2	–	–	3196	3052	4	3	97υ_sCH, Ring C
3	3063 vw	3062 s	3193	3050	6	4	98υ_sCH, Ring A
4	3048 vw	–	3192	3048	6	3	96υ_aCH, Ring C
5	–	–	3191	3047	3	1	95υ_sCH, Ring B
6	–	–	3188	3045	4	0	99υ_aCH, Ring A
7	–	–	3186	3042	7	1	96υ_aCH, Ring B
8	–	–	3183	3040	3	1	95υ_aCH, Rings B–C
9	–	–	3182	3039	1	1	98υ_aCH, Ring A
10	–	–	3176	3033	0	1	95υ_aCH, Ring C
11	–	–	3175	3032	1	1	96υ_aCH, Ring B
12	–	–	3174	3031	2	1	98υ_aCH, Ring A
13	3039 w	–	3168	3025	9	1	97υ_aCH, Ring B
14	–	–	3166	3023	0	0	98υ_aCH, Ring B
15	3023 vw	3023 vw	3165	3022	0	0	98υ_aCH, Ring A
16	3010 vw	3010 vw	3162	3019	2	0	100υ_aCH, Ring B
17	2768 s	2769 m	2876	2747	72	6	100υCH, ald
18	1550 vs	1558 w	1633	1580	100	4	69υOC + 14δHCC + 10υCC
19	–	–	1629	1575	3	4	70υCC + 16δHCC, Ring C
20	–	–	1628	1574	0	4	60υCC + 13δHCC, Ring A
21	–	–	1627	1573	17	4	60υCC + 14δHCC, Ring B
22	–	–	1614	1561	2	1	67υCC + 14δHCC, Ring A
23	–	–	1613	1560	4	1	67υCC + 15δHCC, Ring C
24	1522 vw	–	1608	1555	5	1	66υCC + 12δHCC, Ring B
25	1496 vw	–	1516	1466	5	0	58δHCC + 24υCC, Ring C
26	1480 m	1482 vw	1515	1465	4	0	64δHCC + 23υCC, Ring B
27	–	–	1512	1462	1	0	66δHCC + 25υCC, Ring A
28	1433 s	1420 vw	1468	1420	5	0	33δHCC + 22υCC, Ring A–B–C
29		1409 vw	1467	1419	7	0	42δHCC + 22υCC, Ring A–B–C
30	1396 vw	1394 vw	1465	1417	7	0	48δHCC + 26υCC, Ring A–B–C
31	1378 m	1380 w	1401	1355	10	1	38δHCO + 18υOC + 13υCC + 17δHCC
32	–	–	1368	1323	1	0	70δHCC + 20υCC, Ring B
33	–	–	1357	1312	2	0	59δHCC + 27υCC, Ring C
34	–	–	1350	1306	2	0	52δHCC + 38υCC, Ring A
35	1331 s	–	1336	1292	62	1	34δHCC + 26υCC + 16 δHCP
36	1281 vw	–	1318	1275	1	0	45υCC + 10δHCC, Ring A–B–C
37	–	–	1314	1271	1	0	45υCC, Ring A–B–C
38	1250 vw	–	1311	1267	0	0	62υCC, Ring A–B–C
39	1212 w	–	1218	1178	3	1	72δHCC + 22υCC, Ring B
40	1179 m	1182 w	1211	1171	2	1	72δHCC + 18υCC, Ring C
41	–	–	1205	1165	2	1	74δHCC + 18υCC, Ring A
42	1157 w	1163 w	1186	1147	0	1	76δHCC + 15υCC, Ring C
43	–	–	1185	1146	0	1	75δHCC + 15υCC, Ring B
44	–	–	1184	1145	0	1	75δHCC + 16υCC, Ring A
45	–	–	1120	1083	9	7	41υCC + 19υPC + 18δCCC
46	–	–	1113	1076	13	5	43υCC + 15υPC + 23δCCC
47	1108 s	1108 w	1109	1072	15	4	39υCC + 15υPC + 22δCCC
48	1091 w	1093 m	1104	1068	1	0	40υCC + 34δHCC, Ring C
49	–	–	1104	1067	0	0	44υCC + 35δHCC, Ring B
50	–	–	1100	1063	4	1	38υCC + 36δHCC, Ring A
51	1070 vw	–	1088	1052	17	4	32υCC + 27δHCC + 22δHCP
52	1028 m	1029 m	1048	1013	1	2	53υCC + 27δHCC, Ring B
53	–	–	1047	1013	1	13	54υCC + 24δHCC, Ring C
54	1006 m	–	1046	1011	1	11	59υCC + 33δHCC, Ring A
55	–	–	1034	1000	0	0	90ΓHCCH, Ring B
56	997 vw	1000 s	1016	983	1	17	48ΓHCCH + 21δCCC
57	980 vw	987 vw	1015	982	1	20	24δCCC, Ring C + 11υCC, Ring C + 10γHCCH
58	–	–	1013	979	0	0	46ΓHCCH + 12δCCC
59	–	–	1012	979	0	17	37δCCC + 35υCC, Ring B (trig. Bend)
60	–	–	1012	978	0	4	82γHCCC, Ring C
61	–	–	1007	974	0	2	65γHCCC, Ring A
62	956 vw	955 vw	1002	969	0	0	83γHCCC, Ring B
63	–	–	998	965	0	0	79γHCCC, Ring A
64	–	–	996	963	0	0	80γHCCC, Ring C
65	930 w	934 vw	955	923	0	0	85γHCCC, Ring B
66	–	–	946	914	0	0	91γHCCC Ring A
67	909 vw	–	944	913	0	0	91γHCCC, Ring C
68	854 w	854 vw	874	845	1	0	92γHCCC, Ring B
69	–	–	865	837	0	1	40γHCCC + 20υPC
70	–	–	863	834	0	0	62γHCCC + 19υPC
71	831 s	833 w	855	826	22	9	90γHCCC, Ring C
72	751 s	762 vw	765	740	4	0	64γHCCC, Ring B

(*continued on next page*)

Table 3 (*continued*)

Mode nos.	Experimental wavenumbers (cm^{-1})		Theoretical wavenumbers (cm^{-1}) B3LYP				Assignments PED[c] (%)
	IR	Raman	Unscaled[a]	Scaled[b]	I_{IR}	I_{RAMAN}	
73	–	–	764	739	2	2	39γHCCC, Ring A
74	741 s	741 vw	760	735	12	0	63γHCCC Ring C
75	716 s	719 vw	742	718	14	5	21υPC + 14δOCP + 10γ HCCC
76	692 vs	683 vw	720	697	18	2	23υPC + 18δCCC, Ring A–B–C
77	675 m	–	715	691	7	2	19υPC + 14δCCC, Ring A–B–C
78	–	–	711	688	4	0	43γCCCC + 29γHCCC Ring B
79	–	–	709	685	8	1	42γCCCC + 40γHCCC Ring C
80	668 w	669 m	706	683	9	0	47γCCCC + 35γHCCC Ring A
81	659 vw	643 w	678	655	0	25	23δCCC + 21υPC Ring A–B–C
82	609 vw	618 vw	632	611	0	5	51δCCC + 16δCCH Ring C
83	–	608vw	631	610	0	4	49δCCC + 16δCCH Ring B
84	–	588 vw	631	609	0	3	58δCCC + 20δCCH Ring B
85	556 vw	566 vw	574	555	0	11	51γHCCO + 18γCPCH + 15γγHCCH
86	522 s	528 vw	529	511	34	4	10γCPCC + 10γCCCC
87	509 vs	508 vw	518	501	18	1	31γPCCC
88	488 s	492 vw	498	482	10	1	10γCCCC + 25γCCPC
89	455 m	453 vw	462	447	7	1	15γCCCC + 10υPC
90	446 w	–	445	430	4	1	16γCCCC + 16υPC
91	–	–	411	397	0	1	36γCCCC
92	–	–	407	394	0	0	34γCCCC + 15γCCCH
93	–	–	406	393	0	0	44γCCCC + 17γCCCH
94	–	370 m	373	360	5	11	23δPCC + 136υPC
95	–	344 vw	334	323	5	5	21Γτ OCCP + 15τHCCP + 10υPC + 12τCPCH
96	–	272 w	268	259	1	20	45δCCP + 17υPC
97	–	268 vw	262	253	0	35	43δCCP + 14υPC
98	–	257 s	246	238	0	86	42υPC + 11δCCP
99	–	–	231	223	1	14	11δCPC + 10τCCCC + 10τCCCP
100	–	236 m	225	218	1	39	10τCCCP + 10τOCCP + 10δCPC
101	–	194 m	191	185	0	20	41δCCP + 13τCCCP
102	–	163 s	159	154	3	81	38δCCP++14τCCPC
103	–	107 s	150	145	2	100	25δCCP + 21τCCPC
104	–	92 vs	123	119	1	57	50τCCPC + 25δCCP + 14δCCP
105	–	–	75	72	1	1	42τCCPC + 15δCCP
106	–	–	67	65	1	0	50Γτ CPCC + 15τCCCP
107	–	–	53	52	1	4	41τCPCC + 18δCPC + 10τCCCP
108	–	–	51	49	0	4	27τCPCC + 25Γτ CCCP + 18δCPC
109	–	–	47	45	0	4	84τCPCC
110	–	–	34	33	0	3	88τCPCC
111	–	–	27	26	0	2	89τCPCC

A, B, C: Rings, ν: Stretching, δ: in plane bending, γ: out-of-plane bending, τ: torsional, vs: very strong; s: strong; m: medium; w: weak; vw: very weak.
Relative absorption intensities and Raman intensities normalized with highest peak absorption equal to 100.

[a] Unscaled calculated wavenumbers.

[b] Obtained from the wave numbers calculated at B3LYP/6-31++G(d,p) using scaling factors 0.967 (for wave numbers under 1800 cm^{-1}) and 0.955 (for those over 1800 cm^{-1}).

[c] Total energy distribution calculated B3LYP/6-311++G(d,p) level of theory. Only contributions ⩾10% are listed.

experiments are less than 10 cm^{-1} with a few exceptions. The vibrational bands assignments have been made by using the PED analysis and the animation option of Gauss View 3.0 [39].

4.3.1. C—H vibrations

The aromatic structure shows the presence of C—H stretching vibration in the region 3100–3000 cm^{-1}, which is the characteristic region for the ready identification of C—H stretching vibration [40,41]. In this region, the bands are not affected appreciably by the nature of the substituent. The TPA molecule consists of three benzene ring systems which constitute triphenylphosphonium moiety with P atom. Triphenylphosphonium moiety is bridged to aldehyde group by C1—H2 unit. Hence in our present work, the FT-IR band observed at 3076 was assigned to C1—H2 stretching vibration. The very weak FT-IR bands observed at 3062, 3048, 3039, 3023 and 3010 cm^{-1} and a strong and two very weak FT-Raman bands observed at 3063, 3023 and 3010 cm^{-1} were assigned to aromatic C—H stretching vibrations. For TPA, the C—H stretching vibrations were predicted between 3057 cm^{-1} and 3019 cm^{-1} frequency range for B3LYP/6-31++G(d,p) level of theory. The aromatic C—H in-plane bending vibration occurs in the region 1500–1100 cm^{-1}, and the bands are sharp but have weak-to-medium intensity [41]. The C—H in-plane bending vibrations were observed at 1496, 1480, 1433, 1396, 1331, 1179 and 1157 cm^{-1} in the FT-IR spectrum and at 1482, 1420, 1409, 1394, 1182 and 1163 cm^{-1} in the FT-Raman spectrum. The out-of-plane bending vibrations occur in the wavenumber range 800–1000 cm^{-1} [40]. The bands observed at 956, 930, 909, 854, 831, 751, 741 cm^{-1} in the FT-IR spectrum and the bans observed at 955, 934, 854, 833, 762 and 741 cm^{-1} were assigned to C—H out-of-plane bending vibrations. The calculated wavenumbers of in-plane and out-of-plane CH bands well reproduced the experimental ones in the infrared and Raman spectrum.

4.3.2. Aldehyde group vibrations

The majority of aldehydes show C—H stretching absorbtion in 2830–2695 cm^{-1} region. Two moderately bands are frequently observed in this region. The appearance of two bands is attributed to Fermi resonance between the fundamental aldehydic C—H stretch and the first overtone of the aldehydic C—H bending vibration that usually appears near 1390 cm^{-1}. Only one C—H stretching band is observed for aldehydes, whose C—H bending band has been shifted from 1390 cm^{-1} [42] in FT-IR spectrum. If the intensities of C—H stretching bands are unequal, and if the weaker band is very weak,

as it is seen in our FT-IR spectrum, then the stronger band is nearly pure fundamental [43]. In this study, the medium and sharp band observed at 1378 cm^{-1} in the FT-IR spectrum and the weak band observed at 1380 cm^{-1} in the FT-Raman spectrum were assigned to aldehyde C—H in-plane bending vibrations. The computed value of this vibration is 1355 cm^{-1} in this study. Because this band is shifted from 1390 cm^{-1} to lower wavenumber, the strong band observed at 2768 cm^{-1} in the FT-IR spectrum and the medium band observed at 2769 cm^{-1} in the FT-Raman spectrum were assigned to C—H stretching vibration of aldehyde group in this study. This mode is not contaminated with other vibrations and almost contributing to 100% according to PED.

Aldehydes and ketones show a strong C=O stretching absorption in the region of 1870–1540 cm^{-1}. Its relatively constant position, high intensity, make it one of the easiest bands to be recognized in IR spectra. If a carbonyl group is part of a conjugated system, then the frequency of the carbonyl streching vibration decreases. In addition to this, internal hydrogen bonding shifts the absorption to lover wavenumbers [42,44]. Because of the reasons mentioned above, in our case, the carbonyl stretching vibration was shifted to lower frequency. The very strong band observed at 1550 cm^{-1} in the FT-IR spectrum was assigned to aldehyde C=O stretching vibrations. The same vibration in the FT-Raman spectrum was observed at 1558 cm^{-1} by a very weak band. The calculated value of this band is 1580 cm^{-1}.

4.3.3. P-phenyl group vibrations

When a phenyl group is directly attached to a phosphorous, one of the substituent sensitive phenyl vibrations involves some P—C stretch and it is seen at 1130–1090 cm^{-1} [44]. Clark et al. [45] report that $P(Ph)_3$ have phenyl substituent-sensitive band at 1092 cm^{-1} and a second phenyl substituent-sensitive band at 683 cm^{-1}. This second band also involves some P—C stretch and it is a medium-weak IR band in the region 730–680 cm^{-1}[43,45]. The first substituent-sensitive bands were observed at 1108, cm^{-1} in the FT-IR and FT-Raman spectra in this study. The computed values were good reproduced experimental ones but, according to PED, these vibrations are contaminated with other C—C stretching and bending vibrations. The second P—C stretching bands were observed at 716, 692 and 675 cm^{-1} in the FT-IR spectrum and at 719, 683 cm^{-1} in the FT-Raman spectrum for TPA. Computed values of these bands are 718, 697 and 691 cm^{-1} in this study.

4.3.4. C=C vibrations

In the present work, the frequencies observed in the FT-IR spectrum at 1522, 1281, 1250, 1091, 1070, 1028 and 1006 cm^{-1} and the bands observed at 1093 and 1029 cm^{-1} in the FT-Raman spectrum were assigned to C—C stretching vibrations. According to the PED analysis, the computed values of mode no 57, 59, 81, 82, 83 and 84 which values are 982, 979, 655, 611, 610 and 609 cm^{-1} are related to the C—C—C bending vibrations. The bands observed at 980, 659, 609 cm^{-1} in the FT-IR spectrum and the bands observed at 987, 643, 618, 608 and 588 cm^{-1} in the FT-Raman spectrum were assigned to C—C—C bending vibrations. The theoretically computed C—C—C out-of-plane and in-plane bending vibrational modes have been found to be consistent with recorded spectral values. The PED of these vibrations are not pure modes as it is evident from the last column of PED in Table 3.

5. Conclusion

The FT-IR and FT-Raman spectra were studied. The equilibrium geometries, harmonic wavenumbers, ground state energy, and dipole moment of TPA were calculated for the first time. Optimized geometrical parameters of the title compound are in agreement with the crystal structure data obtained from XRD studies. All calculations were shown good correlation with the experimental data. The calculated vibrational values are in good agreement when they are compared with IR and Raman experimental data. *Ab initio* programs were used to find the most stable conformer of TPA.

Acknowledgment

This work was financially supported by the BAP (Project Number: 11401012), Selcuk University in Turkey.

References

[1] G. Wittig, U. Schöllkopf, Chem. Ber. 87 (1954) 1318.
[2] G. Wittig, W. Haag, Chem. Ber. 88 (1955) 1654.
[3] D. Rideout, T. Calogeropoulou, J.S. Jaworski, R. Dagnino, M.R. McCarthy, Anti-Cancer Drug Des. 4 (1989) 265.
[4] C.V. Coulter, G.F. Kelso, Tsu-Kung Lýn, R, A.J. Smýth, M.P. Murphy, Free Radic. Biol. Med. 28 (2000) 1547.
[5] M.P. Murphy, R.A.J. Smith, Adv. Drug Deliv. Rev. 41 (2000) 235.
[6] W.A. Cooper, W.A. Bartier, D.C. Rideout, E.J. Delikatny, Magn. Reson. Med. 45 (2001) 1001.
[7] El-R. Kenawy, F.I. Abdel-Hay, L. Shahada, Abd El-Raheem R. El-Shanshoury, M.H. El-Newehy, J. Appl. Polym. Sci. 102 (2006) 4780.
[8] M. Shafiq, I.U. Khan, M.N. Tahir, W.A. Siddiqui, Acta Cryst. E64 (2008) 558.
[9] M.N. Tahir, M. Shafiq, I.U. Khan, W.A. Siddiqui, M.N. Arshad, Acta Cryst. E64 (2008) 557.
[10] R.J. Dubios, C.C.L. Lin, J. Med. Chem. 21 (1978) 303.
[11] J. Patel, D. Rideout, M.R. McCarthy, T. Calogeropoulou, K.S. Wadwa, A.R. Oseroff, Anticancer Res. 14 (1994) 21.
[12] A. Manetta, G. Gamboa, A. Nasseri, Y.D. Podnos, D. Emma, G. Dorion, L. Rawlings, P.M. Carpenter, A. Bustamante, J. Patel, D. Rideout, Gynecol. Oncol. 60 (1996) 203.
[13] E.J. Delikatny, S.K. Roman, R. Hancock, T.M. Jeitner, C.M. Lander, D.C. Rideout, C.E. Mountford, Int. J. Cancer 67 (1996) 72.
[14] Z.W. Lou, X.M. Shang, Chin. J. Med. Chem. 10 (2000) 168.
[15] J.J. Fu, L.H. Yan, Y.Y. Wang, Jiangsu Chem. Ind. 31 (6) (2003) 12 (in Chinese).
[16] S.H. Mashraqui, R.S. Kenny, S.G. Ghadigaonkar, A. Krishnan, M. Bhattacharya, Opt. Mater. 27 (2004) 257.
[17] S. Ishikawa, K. Manabe, J. Chem. Soc. Chem. Commun. (2006) 2589.
[18] W. Deng-Yu, L. Fang-Shi, X. Jin-Yun, M. Nan-Wen, Y. Hong-Liang, Acta Cryst. E63 (2007) o4532.
[19] J.U. Calderon, B. Lennox, M.R. Kamal, Appl. Clay Sci. 40 (2008) 90.
[20] N. Sundaraganesan, B. Anand, C. Meganathan, B.D. Joshua, Spectrochim. Acta A 68 (2007) 561.
[21] M.K. Subramanian, P.M. Anbarasana, S. Manimegalaia, J. Raman Spectrosc. 40 (2009) 1657.
[22] V. Krishnakumar, N. Jayamani, R. Mathammal, K. Parasuramand, J. Raman Spectrosc. 40 (2009) 1551.
[23] P.J. O'Malley, J. Mol. Struct.: Theochem. 755 (2005) 147.
[24] J. Karpagam, N. Sundaraganesan, S. Kalaichelvan, S. Sebastian, Spectrochim. Acta Part A 76 (2010) 502.
[25] S. Sebastian, N. Sundaraganesan, Spectrochim. Acta Part A 75 (2010) 94.
[26] Y. Erdogdu, O. Unsalan, M. Amalanathan, I.H. Joe, J. Mol. Struc. 980 (2010) 24–30.
[27] Ö. Dereli, S. Sudha, N. Sundaraganesan, J. Mol. Struc. 994 (2011) 379–386.
[28] P. Chinna Babu, N. Sundaraganesan, Ö. Dereli, E. Türkkan, Spectrochim. Acta Part A 79 (2011) 562–569.
[29] N. Subramanian, N. Sundaraganesan, Ö. Dereli, E. Türkkan, Spectrochim. Acta Part A 83 (2011) 165.
[30] R.H. Clark, C.D. Flint, A.J. Hempleman, Spectrochim. Acta Part A 43 (1987) 805.
[31] M. Geoffroy, G. Rao, Z. Tancic, G. Bernardinelli, J. Am. Chem. Soc. 112 (1990) 2826–2827.
[32] Spartan 08, Wavefunction Inc., Irvine, CA 92612, USA, 2008.
[33] Gaussian 03, Revision E.01, M.J. Frisch, G.W. Trucks, H.B. Schlegel, G.E. Scuseria, M.A. Robb, J.R. Cheeseman, J.A. Montgomery, Jr., T. Vreven, K.N. Kudin, J.C. Burant, J.M. Millam, S.S. Iyengar, J. Tomasi, V. Barone, B. Mennucci, M. Cossi, G. Scalmani, N. Rega,G.A. Petersson, H. Nakatsuji, M. Hada, M. Ehara, K. Toyota, R. Fukuda, J. asegawa, M. Ishida, T. Nakajima, Y. Honda, O. Kitao, H. Nakai, M. Klene, X. Li, J.E. Knox, H. P. Hratchian, J.B. Cross, C. Adamo, J. Jaramillo, R. Gomperts, R.E. Stratmann, O. Yazyev,A.J. Austin, R. Cammi, C. Pomelli, J.W. Ochterski, P.Y. Ayala, K. Morokuma, G.A. Voth, P. Salvador, J.J. Dannenberg, V.G. Zakrzewski, S. Dapprich, A.D. Daniels, M.C. Strain, O. Farkas, D.K. Malick, A.D. Rabuck, K. Raghavachari, J.B. Foresman, J.V. Ortiz, Q. Cui, A.G. Baboul, S. Clifford, J. ioslowski, B.B. Stefanov, G. Liu, A. Liashenko, P. Piskorz, I. Komaromi, R.L. Martin, D.J. Fox, T. Keith, M.A. Al-Laham, C.Y. Peng, A. Nanayakkara, M. Challacombe, P.M.W. Gill, B. Johnson, W. Chen, M.W. Wong, C. Gonzalez, J.A. Pople, Gaussian, Inc., Pittsburgh, PA, 2003.
[34] H.B. Schlegel, J. Comput. Chem. 3 (1982) 214.

[35] A. Frisch, A.B. Nielson, A.J. Holder, Gaussview User Manual, Gaussian Inc., Pittsburgh, PA, 2000.
[36] G. Rauhut, P. Pulay, J. Phys. Chem. 99 (1995) 3093.
[37] R. Wysokinski, K. Hernik, R. Szostak, D. Michalska, Chem. Phys. 333 (2007) 37–48.
[38] Y. Erdogdu, O. Unsalan, D. Sajan, M.T. Gulluoglu, Spectrochim. Acta Part A 76 (2010) 130–136.
[39] Gauss View, Version 4.01, Dennington II, Roy, T. Keith, J. Millam, K. Eppinnett, W.L. Hovell, R. Gilliland, Semichem, Inc., Shawnee Mission, KS, 2003.
[40] G. Varsanyi, Assignments for Vibrational Spectra of Seven Hundred Benzene Derivatives, vols. 1 and 2, Academic Kiado, Budapest, 1973.
[41] M. Jag, Organic Spectroscopy – Principles and Applications, second ed., Narosa Publishing House, New Delhi, 2001.
[42] R.M. Silverstein, F.X. Webster, D.J. Kiemle, Spectrometric Identification of Organic Compounds, seventh ed., John Wiley & Sons, New York, 2005.
[43] D.L. Vien, N.B. Colthup, W.G. Fateley, J.G. Grasselli, The Handbook of Infrared and Raman Characteristic Frequencies of Organic Molecules, Academic Press, Boston, 1991.
[44] G. Socrates, Infrared and Raman Characteristic Group Frequencies, third ed., John Wiley & Sons, New York, 2004.
[45] R.H. Clark, C.D. Flint, A.J. Hempleman, Spectrochim. Acta 43 A (1987) 805.